Inorganic Chemistry

pubs.acs.org/IC Article

An Integrated View of Nitrogen Oxyanion Deoxygenation in Solution Chemistry and Electrospray Ion Production

Daniel M. Beagan, Alyssa C. Cabelof, Robert Pepin, Maren Pink, Veronica Carta, and Kenneth G. Caulton*



Cite This: Inorg. Chem. 2021, 60, 17241-17248



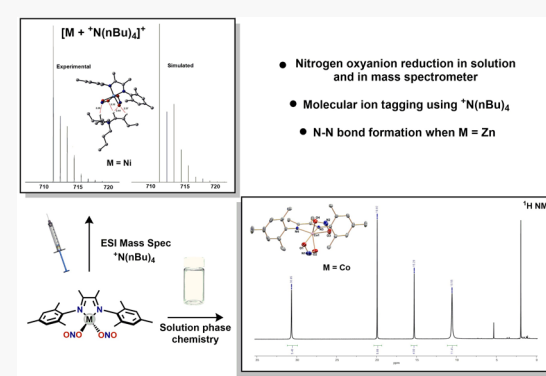
ACCESS

III Metrics & More

Article Recommendations

SI Supporting Information

ABSTRACT: There has been an increasing interest in chemistry involving nitrogen oxyanions, largely due to the environmental hazards associated with increased concentrations of these anions leading to eutrophication and aquatic "dead zones". Herein, we report the synthesis and characterization of a suite of MNO_x complexes (M = Co, Zn: x = 2, 3). Reductive deoxygenation of cobalt bis(nitrite) complexes with bis(boryl)pyrazine is faster for cobalt than previously reported nickel, and pendant O-bound nitrito ligand is still readily deoxygenated, despite potential implication of an isonitrosyl primary product. Deoxygenation of zinc oxyanion complexes is also facile, despite zinc being unable to stabilize a nitrosyl ligand, with liberation of nitric oxide and nitrous oxide, indicating N–N bond formation. X-ray photoelectron spectroscopy is effective for discriminating the types of nitrogen in these molecules. ESI mass spectrometry of a suite of M(NO_x)_y (x = 2, 3 and y = 1, 2) shows that the primary form of ionization is loss of an



oxyanion ligand, which can be alleviated via the addition of tetrabutylammonium (TBA) as a nonintuitive cation pair for the neutral oxyanion complexes. We have shown these complexes to be subject to deoxygenation, and there is evidence for nitrogen oxyanion reduction in several cases in the ESI plume. The attractive force between cation and neutral is explored experimentally and computationally and attributed to hydrogen bonding of the nitrogen oxyanion ligands with ammonium α -CH₂ protons. One example of ESI-induced reductive dimerization is mimicked by bulk solution synthesis, and that product is characterized by X-ray diffraction to contain two Co(NO)₂⁺ groups linked by a highly conjugated diazapolyene.

■ INTRODUCTION

The increase in anthropogenically derived nitrogen oxyanions has led to a variety of economic and environmental problems, including large algal blooms in eutrophic bodies of water, inducing hypoxia and often leading to dead zones. ^{1–6} Mitigation of this eutrophication has been approached through photochemical, ^{7–10} electrochemical, ^{11–15} and chemical reduction of nitrogen oxyanions. ^{16–24} One approach involves reductive borylation (Scheme 1) where equimolar bis(boryl)-

Scheme 1. Generic Reductive Borylation of a Metal Nitrate Complex to Afford a Metal Nitrite, along with Boryl Ether and Pyrazine

pyrazine reagent removes oxygen, as (Bpin)₂O, because of the affinity of boron for oxygen. Our group has recently shown several examples of reductive deoxygenation using reduced N-heterocycles, ^{25–28} including deoxygenation of a nickel complex to induce N–N bond formation. ²⁹

To gain a better understanding of molecular nitrogen oxyanion chemistry, we have synthesized a suite of (DIM)M- $(NO_x)_2$ complexes (DIM = N,N'-bis(2,4,6-trimethylphenyl)-1,4-diaza-2,3-dimethyl-1,3-butadiene) M = Co, Zn; x = 2, 3) to probe structural and spectroscopic similarities, which we also compare to previously reported (DIM)Fe $(NO_x)_2$ (x = 1, 3) and (DIM)Ni $(NO_x)_2$ (x = 2, 3). DIM is a redox-active bidentate ligand with desirable steric bulk in its mesityl arms. x = 300-32 Although IR, NMR, and X-ray photoelectron spectroscopy (XPS) can all be useful in distinguishing between

Received: August 22, 2021 Published: October 27, 2021





complexes of different metals and oxidation states of the coordinated nitrogen oxides, mass spectrometry of these compounds often favors loss of an oxyanion ligand, which precludes identification of the molecular species. Loss of an Xtype ligand must be avoided when other characterization techniques are insensitive to those: for example, ¹⁵N NMRsilent paramagnetic complexes. The ability to see an intact molecular ion with a complex that has nitrogen oxyanion ligands is increasingly important for characterizing subsequent reactivity and was a hindrance in a previous study with a nickel nitrogen oxyanion complex (see the Supporting Information). We report here a useful advance in such detection of the intact molecule using ESI mass spectrometry via the nonintuitive pairing of neutral oxyanion complexes with a tetrabutylammonium cation. Furthermore, we study the impact of the metal center on the reduced nitrogen containing products following deoxygenation of the bis(nitrate) and bis(nitrite) complexes reported here.

RESULTS AND DISCUSSION

The (DIM)MCl₂ (M = Zn, Co) complexes were synthesized via addition of DIM to a stirring solution of the corresponding metal halide salt in THF for 12 h. Starting with these dichloride complexes, the bis(nitrite) and bis(nitrate) complexes were synthesized by using the appropriate silver salt. For Zn, the addition of silver nitrate or nitrite to a stirring solution of the dichloride starting material at room temperature resulted in the immediate precipitation of silver chloride, and work-up gave the bis(nitrate) and bis(nitrite) complexes in high yields. For Co, room temperature addition of AgNO2 or AgNO3 to (DIM)CoCl₂ results in partial salt metathesis, along with partial oxidation to Co(III), as established by ¹H NMR spectroscopy. The reducing power of CoII makes it vulnerable in the presence of Ag^+ . However, when repeated at -35 °C, (DIM)Co(NO₃)₂ and (DIM)Co(NO₂)₂ can be synthesized and isolated in high yields. The synthesis of the (DIM)M- $(NO_x)_2$ complexes (M = Co, Zn; x = 2, 3) is summarized in Scheme 2.

Scheme 2. Synthetic Route to Varied DIM Metal Nitrate and Nitrite Complexes

All of the complexes shown in Scheme 2 were characterized by NMR and IR spectroscopy (Figures S3–S6 and S12–S17) and are fully consistent with the bis(nitrate) or bis(nitrite) identity. Further characterization was completed by single crystal X-ray diffraction, and the molecular structures are shown in Figure 1.

(DIM)Co(NO₃)₂ and (DIM)Co(NO₂)₂ are paramagnetic complexes with idealized 2-fold symmetry based on four 1 H NMR resonances, with appropriate intensities and a chemical shift range from +31 to +10 ppm. Each is pseudo-octahedral, with one long (2.17–2.20 Å) and one short (2.05–2.09 Å)

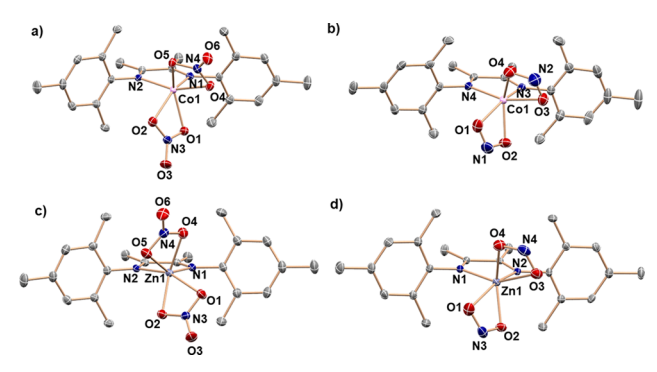


Figure 1. ORTEP representation of the molecular structures (50% probabilities) of the non-hydrogen atoms of $(DIM)M(NO_x)_2$ for M = Co and Zn and x = 2 or 3. Selected structural parameters (Å): For (a) Co1-N1, 2.0694(18); Co1-N2, 2.0640(17); Co1-O2, 2.1706(16); Co1-O4, 2.1740(15); Co1-O5 2.085315); Co1-O1, 2.0968(15); O1-N3, 1.273(2); O2-N3, 1.264(2); O5-N4, 1.286(2); O6-N4, 1.216(2); O3-N3, 1.225(2); O4-N4, 1.267(2). For (b) Co1-O1, 2.1925(11); Co1-O3, 2.2052(11); Co1-N3, 2.0996(11); Co1-N4, 2.0904(11); Co1-O2, 2.0531(12); Co1-O4, 2.0592(11); O1-N1, 1.257(2); O3-N2, 1.246(2); O2-N1, 1.274(2); O2-N4, 1.2688(19). For (c) Zn1-N1, 2.070(2); Zn1-N2, 2.0635(19); Zn1-O2, 2.0910(18); Zn1-O4, 2.1277(19); Zn1-O5 2.202(2); Zn1-O1, 2.2171(19); O1-N3, 1.264(3); O2-N3, 1.277(3); O5-N4, 1.260(3); O6-N4, 1.220(3); O3-N3, 1.220(3); O4-N4, 1.279(3). For (d) Zn1-O2, 2.0471(17); Zn1-O4, 2.0606(19); Zn1-N1, 2.0887(18); Zn1-N2, 2.0939(18); Zn1-O3, 2.3004(18); Zn1-O1, 2.3243(19); N3-O1, 1.240(3); N3-O2, 1.286(3); N4-O3, 1.249(3); N4-O4, 1.268(3).

Co-O distance. The long Co-O contacts are well within the sum of the van der Waals radii (3.44 Å). The bis(nitrate) is comparable to other cobalt bis(nitrate) complexes with two other ancillary donors. 33-35 Cobalt bis(nitrite) complexes are usually N-bound and six-coordinate, 36-39 and we hypothesize the nitrite ligands are O-bound in $(DIM)Co(NO_2)_2$ to accommodate bidentate binding and provide a six-coordinate environment about the cobalt center. The structure of the zinc bis(nitrate) has two bidentate nitrates, each with one long (2.22 Å) and one short (2.09 Å) Zn-O distance. The zinc bis(nitrite) is O-bound and bidentate, again each with one long (2.32 Å) and one short (2.05 Å) Zn-O distance per nitrite. These zinc complexes might be described as four-coordinate, tetrahedral zinc, with weak donation from the pendant oxygen nucleophile, but the weak interactions are stronger in the bis(nitrate) complex. Each long Zn-O distance is within the sum of the van der Waals radii (2.91 Å). In all four molecules, the longer M-O distances are in the DIM NCCN plane, trans to the DIM nitrogens.

Deoxygenation Reactivity Studies. *Cobalt.* After reporting different reduced products for bis(oxyanion) complexes coordinated to iron and nickel, we were interested in the reductive deoxygenation of a cobalt complex bearing two nitrogen oxyanion ligands. We hypothesized that the formation of a cobalt dinitrosyl complex was possible; however, most reported $Co(NO)_2$ complexes with neutral ancillary donors are monocationic to invoke $\{Co(NO)_2\}^{10}$ in the Enemark–Feltham notation.

Reaction of equimolar (Bpin)₂Pz with (DIM)Co(NO₂)₂ in THF proceeds (Scheme 3) in time of mixing at 25 °C, with a color change from brown to purple. Complete consumption of the cobalt starting material and of the boryl reagent is observed, as well as the formation of (Bpin)₂O₂, to yield a

Scheme 3. Synthesis of (DIM)Co(NO)(ONO)

paramagnetic product (Figure S7) which shows $\nu_{\rm NO}$ at 1723 cm⁻¹ (Figure S8), similar to other cobalt nitrosyl complexes with a linear NO ligand. After removal of organic byproducts by rinsing with pentane, crystals suitable for X-ray diffraction were obtained, and the molecular structure confirms (Figure 2) the formation of (DIM)Co(NO)(ONO),

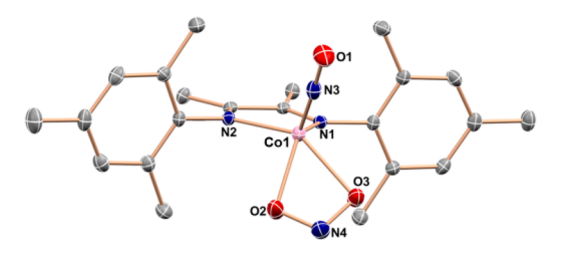


Figure 2. ORTEP representation of the molecular structure (50% probabilities) of the non-hydrogen atoms of (DIM)Co(NO)(ONO), showing selected atom labeling. Selected structural parameters (Å): Co1–N3, 1.665(2); Co1–N1, 2.0125(19); Co1–N2, 2.0417(18); Co1–O2, 2.0942(17); Co1–O3, 2.2072(17); O1–N3, 1.180(3); O2–N4, 1.263(3); O3–N4, 1.259(3).

which has no crystallographic symmetry but is pseudo-square-pyramidal about the cobalt metal center. The nitrito ligand is bidentate, albeit with the Co–O3 distance longer by 0.11 Å. The kinetically facile deoxygenation of $(DIM)Co(NO_2)_2$ contrasts the nickel analogue, which requires 12 h at room temperature to completely deoxygenate. Furthermore, while N_2O was observed for subsequent deoxygenations using nickel, no N_2O was observed for the cobalt deoxygenations.

Ignoring donation from the more distant oxygen, (DIM)-Co(NO)(ONO) would have 17 valence electrons, which justifies additional donation from another oxygen but not a truly bidentate (equal Co-O distances) nitrito ligand, which would be a 19 valence electron species. The Co-N-O nitrosyl bond angle is linear (174.26°), indicating NO+, and Enemark-Feltham designation {CoNO}.9 The bond lengths within the α -diimine backbone indicate increased electron density, evidenced by contraction of the C-C bond and lengthening of the C-N bonds as compared to other DIM containing species reported. The C-C bond in (DIM)Co(NO)(ONO) is 0.037 and 0.041 Å shorter than in the cobalt bis(nitrite) and bis(nitrate) analogues and is 0.043 Å shorter than the C-C bond in both zinc structures (zinc should be most indicative of completely unreduced DIM). While there is a smaller change in the C-N bonds compared to (DIM)Zn(NO₂)₂, the (DIM)Co(NO)(ONO) C-N distances are lengthened by 0.014 and 0.019 Å. These bond lengths indicate participation of (CoNO)2+ with a reduced DIM ligand backbone, as opposed to purely (CoNO)+ with neutral DIM (Table S1). Cobalt here is more reducing than in the (DIM)Ni(NO)-(ONO) analogue, as judged by bond lengths within DIM.

Zinc. With zinc lacking the ability to coordinate the π -acidic nitrosyl ligand, we were interested in single deoxygenation of (DIM)Zn(NO₂)₂. The reaction of an equimolar solution of (DIM)Zn(NO₂)₂ with (Bpin)₂Pz shows only partial con-

sumption of $(DIM)Zn(NO_2)_2$ by 1H NMR, along with the formation of pyrazine, $(Bpin)_2O$, and free DIM ligand. When executed in a 2:5 molar ratio of $(DIM)Zn(NO_2)_2$ to $(Bpin)_2Pz$, complete consumption of both starting materials is observed as well as formation of pyrazine, $(Bpin)_2O$, and free ligand with appropriate intensities (Scheme 4) as judged by 1H

Scheme 4. Deoxygenation of $(DIM)Zn(ONO)_2$ with $(Bpin)_2Pz$

NMR (Figure S19). Transfer of the headspace volatiles, after 12 h of reacting in MeCN, into a gas IR cell shows formation of N_2O and NO in the IR spectrum (Figure 3). The N_2O

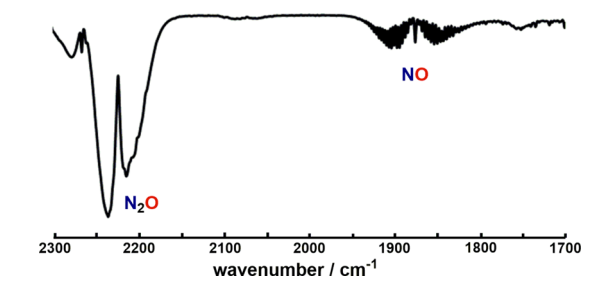


Figure 3. Gas-phase IR spectrum of the headspace after the reaction of $(DIM)Zn(ONO)_2$ and $(Bpin)_2Pz$ showing the formation of N_2O (2224 cm⁻¹) and NO (1864 cm⁻¹).

absorption at 2224 cm $^{-1}$ is greater in intensity than the NO absorption at 1872 cm $^{-1}$, despite the balanced reaction producing 2 mol of NO and only 1 mol of N₂O. This is consistent with the molar absorptivity of the vibration at 2224 cm $^{-1}$ for N₂O being about 8 times greater than that of the absorption at 1872 cm $^{-1}$ for NO.

The loss of NO and N₂O from this reaction can be attributed to the inability of zinc to coordinate a nitrosyl ligand, and the N–N bond formation most likely happens after formation of a high-energy Zn-NO intermediate, formed via single deoxygenation of (DIM)Zn(NO₂)₂. The zinc metal product has been confirmed by XPS (Figure S22). Importantly, the 2 NO, 2 DIM, and 2 Zn are the same constituent parts of the previously reported nickel dimer [(DIM)Ni(NO)]₂; ²⁶ however, replacing nickel with zinc drastically changes the arrangement of these constituent parts. Instead of being held together in a M–M dimer, the reactivity with zinc shows free nitric oxide, uncoordinated DIM ligand, and zinc metal.

The analogous reactivity can be accomplished starting from (DIM)Zn(NO₃)₂, although heating at 80 °C in MeCN is required (Figure S20). The room temperature reactivity of (DIM)Zn(NO₂)₂ and heat required for reactivity with (DIM)Zn(NO₃)₂ is analogous to the trend for nickel complexes. The heating required for the bis(nitrate) complexes indicates kinetic barriers associated with nitrate reduction, despite favorable reduction potentials. 48

X-ray Photoelectron Spectroscopy (XPS). XPS can be a valuable technique for distinguishing between different nitrogen oxyanions, and we were interested in looking at our NO_x⁻ complexes to see if XPS could resolve nitrogens of varied oxidation states. The data for the bis(nitrate) and bis(nitrite)

complexes show clear resolution of both nitrate/nitrite nitrogen from the DIM imine nitrogens (400 eV) in the N 1s region (Figure S21). Each bis(nitrate) complex has a binding energy (BE) of 407 eV, while the bis(nitrite) complexes have a BE of 403.5 eV, consistent with easier ionization in trivalent nitrite. In general, the experimental atom ratios for nitrate or nitrite nitrogens compared to DIM ligand nitrogens is 1:1, consistent with expectations. The XPS data for these compounds also suggest that slight changes in denticity of the oxyanion ligand are undetectable by XPS.

Mass Spectrometry of DIM Nitrogen Oxyanion Complexes. We found that the electrospray ionization, ESI(+), mass spectrum of (DIM)Ni(NO)(ONO) in THF shows mainly ions involving loss of the nitrito ligand; there is no intact molecular ion. However, upon addition of tetrabutylammonium ion (TBA) to a THF solution of (DIM)Ni(NO)-(ONO), species $[(DIM)Ni(NO)(ONO)\cdot TBA]^+$ is the most intense signal (Figure S25). With TBA generally being considered a noncoordinating cation, we were interested in the nature of this nonintuitive (cation with neutral) interaction between TBA and (DIM)Ni(NO)(ONO). Furthermore, to understand if two NO_x^- ligands were necessary to form a molecular TBA adduct, we synthesized an analogue of (DIM)Ni(NO)(ONO) bearing only one oxyanion ligand. The nitrosyl complex (DIM)Ni(NO)(Br) was synthesized via nitrosylation of the Ni(I) dimer, $[(DIM)NiBr]_2$ (Scheme 5).

Scheme 5. Synthesis of (DIM)Ni(NO)(Br) from [(DIM)NiBr], and NO Gas

Addition of excess NO to a stirring solution of [(DIM)NiBr]₂, which was synthesized according to the literature procedures, in ether resulted in an immediate color change from deep purple to green, along with precipitation of a green solid. After workup, ¹H NMR spectroscopy (Figure S18) indicates clean conversion to the diamagnetic (DIM)Ni(NO)(Br), assigned as {NiNO}, ¹⁰ which was confirmed by single-crystal X-ray diffraction (Figure 4). We also obtained ESI+ mass spectrometry data on (DIM)NiBr₂ as a control with no nitrogen oxyanion ligands.

Mass Spectrometry in the Absence of TBA. Before attempting to form TBA adducts with the various DIM complexes, we obtained ESI+ mass spectral data on each of the complexes in THF in the absence of added TBA. For the nickel complexes (DIM)Ni(NO₂)₂ (Figure S28), (DIM)Ni-(NO₃)₂ (Figure S26), (DIM)Ni(NO)(Br) (Figure S37), and (DIM)NiBr₂ (Figure S39), the most intense signals in the ESI + mass spectra are the resultant cation after loss of nitrite, nitrate, or bromide, with no detectable intensity of the intact molecular ion. For simplicity across samples, we have chosen to denote the intact molecule as "Q". For example, the loss of a nitrite ligand from (DIM)Ni(NO₂)₂ would be denoted as [Q - NO₂]⁺ (molecule minus nitrite). The (DIM)NiX⁺ cation formed after ligand loss is Lewis acidic, which leads to dimerization in the spectrometer with a neutral complex to give the observed m/z for $[2Q - NO_x]^+$. This type of

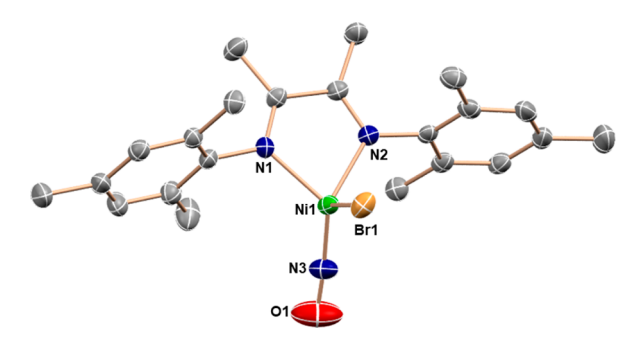


Figure 4. ORTEP representation of the molecular structure (50% probabilities) of (DIM)Ni(NO)(Br) showing selected atom labeling. Selected structural parameters (Å, deg): Ni1–Br1, 2.4120(6); Ni1–N1, 2.004(3); Ni1–N2, 2.017(3); Ni1–N3, 1.639(3); N3–O1, 1.152(4); O1–N3, 1.180(3); Ni1–N3–O1, 175.7(4).

monocation dimer has been reported with nitrite as the bridging ligand between two nickel centers. ⁵⁰ DIM transfer is also a common occurrence, producing $[(DIM)_2MNO_x]^+$, a product of DIM ligand redistribution.

In contrast to these nonredox processes, redox at nitrogen accounts for the other ions detected; such processes are thus relevant to the general goal here of NO_x^- deoxygenation. These processes are inevitably reduction of nitrogen and attributed to hydrogen atom transfer (HAT) from the electrospray plume, with the THF solvent as the HAT reductant. For example, the $[2Q - NO_2]^+$ ions for (DIM)- $M(ONO)_2$ with M = Co, Ni, and Zn also show loss of mass 29, followed by a second loss of 29 (Figures S28, S32, and S35). Isotope multiplet simulation clearly rules out loss of mass 30 (nitric oxide) in these two steps. We attribute these to loss of NO accompanied by addition of a hydrogen atom (the hydrogen originating from reducing agent THF in the electrospray environment). The loss of NO was confirmed by the expected mass shift observed when sampling (DIM)- $Ni(O^{15}NO)_2$. The -29 process is predictably absent for (DIM)NiBr₂. In brief, this process replaces NO in ON^{III}O⁻ by H, forming OH-. These two steps of reductive elimination of neutral NO and H atom addition do not involve redox chemistry at the metal center (ONO $^-$ + H \rightarrow OH $^-$ + NO); this overall redox-neutral character makes this an energetically viable source of monocations. The reduction of nitrite to nitric oxide, followed by H atom transfer to form a hydroxide ligand, has been observed for copper,⁵¹ and nitric oxide liberation liberation from nitrite upon deoxygenation has also been reported.^{21,52,53}

Zinc provides key information about processes favored when the metal offers no redox change. From (DIM)Zn(NO₃)₂, only ions carrying nitrite are observed (Figure S34), suggesting nitrate deoxygenation in the spectrometer aided by the Lewis acidic Zn²⁺ metal center. After deoxygenation, the traditional Zn²⁺ ion, $[(DIM)_2Zn_2(NO_2)_3]^+$, is seen together with $[(DIM)_2Zn_2(NO_2)_2(OH)]^+$, similar to the bis(nitrite) complexes above.

The molecule (DIM)Co(NO)(ONO) behaves very differently from its nickel analogue, and the ESI chemistry is best understood as producing an energetically preferred cobalt dinitrosyl. The molecular ion Q^+ is absent, and the dominant species is $[Q-O]^+$, which is the 18-electron $[(DIM)Co(NO)_2]^+$ (Figure S38). An equally dominant species is $[2Q-2H_2O]^+$. This dicobalt species $[(DIM-2H)Co(NO)_2]_2^+$ is suggested to have lost two hydrogens per DIM, together with

carbon-carbon bond coupling (Scheme 6), yielding two of the 18-electron Co(NO)₂⁺ species linked by a now-tetradentate

Scheme 6. Proposed C–C Coupling of Dehydrogenated DIM in Observed [(DIM-2H)Co(NO)₂]₂⁺

dianionic diimine ligand. In summary, it is the 18-valence-electron $Co(NO)_2^+$ species that gives the highest yield of ions. The ion corresponding to loss of a nitrite ligand to yield $[Q-NO_2]^+$ is also present, but with much lower intensity.

Solution Deoxygenation Chemistry Mimics ESI Reactivity. This tendency of DIM methyl groups to function as H atom donors is also detected by reaction chemistry. In an effort to synthesize a cobalt dinitrosyl complex, the addition of $(Bpin)_2Pz$ to $(DIM)Co(ONO)_2$ in a 2:1 mole ratio results in an immediate color change from brown to purple, which persists after 12 h of stirring at room temperature. All $(Bpin)_2Pz$ and the paramagnetic $(DIM)Co(ONO)_2$ starting reagent have been completely consumed. After removal of the THF in vacuo, the purple solid was redissolved in a minimal amount of ether and held at -35 °C, giving black needles after 12 h. The molecular structure (Figure 5) corresponds to

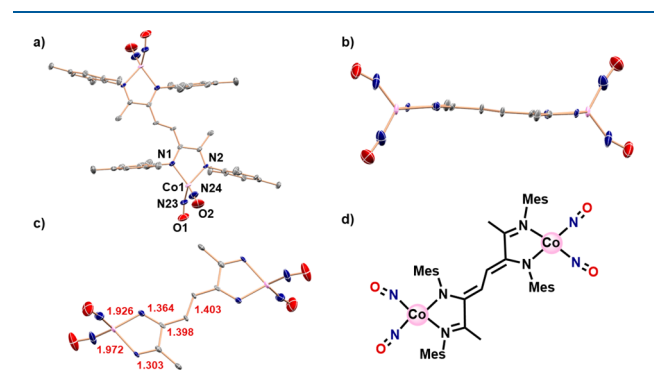


Figure 5. (a) ORTEP representation (50% probabilities) of the molecular structure of the non-hydrogen atoms of [(DIM – 2H)Co(NO)₂]₂, showing selected atom labeling. Selected structural parameters (Å, deg): Co1–N1, 1.660; Co1–N2, 1.637; N1–O1, 1.147; N2–O2, 1.149; Co1–N23–O1, 154.95; Co1–N24–O2, 172.82. (b) Side view showing planarity due to complete conjugation across the dimer. (c) Top-down view showing bond lengths in the Co(DIM) fragment (unlabeled bond lengths are symmetry equivalent by an inversion center). (d) Dominant resonance structure based on bond lengths.

dimeric $[(DIM-2H)Co(NO)_2]_2$, where two $(DIM-2H)Co(NO)_2$ units couple through the doubly H atom abstracted $-CH_3$ group on the DIM backbone. In the isolated $[(DIM-2H)Co(NO)_2]_2$ complex, since the (2DIM-4H) ligand is now a conjugated dianion (Figure 5d), each cobalt has achieved an 18-electron configuration in its $Co(NO)_2^+$ unit. The anticipated neutral $(DIM)Co(NO)_2$ would have 19 valence electrons, and charge leakage into the DIM backbone would help rationalize the observed allylic radical reactivity at the DIM $-CH_3$ group. The C-C coupling observed has literature precedence with similar systems. S4,555 Because the uncharged moiety $Co(NO)_2$ is unknown, but its cation is known, double dehydrogenation of a DIM methyl, then

dimerization, achieves conjugation over eight atoms, in addition to achieving the preferred even electron Co(NO)_2^+ . Reductive borylation replicates what is seen in the ESI mass spectrum.

Impact of $N(N-Bu)_4^+$ on ESI Ion Production. Before surveying the nitrogen oxyanion complexes for their ability to form TBA adducts in the mass spectrometer, we sought an appropriate ratio of metal complex to TBA, as its iodide salt. We found that TBA in the $10-20~\mu M$ range with metal complex in the 1-5~mM range allowed for the highest intensity of TBA-adduct formation. With higher concentrations of TBAI present, the spectra were dominated by $(TBA)_xI_{x-1}$ clusters.

The addition of [TBA]I to (DIM)Ni(NO₂)₂ results in the [Q + TBA]⁺ as the most intense species in the mass spectrum (Figure S29). All species seen without the TBA additive are still present, but at much lower intensities. Similarly, additions of [TBA]I to (DIM)Ni(NO₃)₂, (DIM)Ni(NO)(Br), (DIM)-Co(NO₃)₂, (DIM)Co(NO₂)₂, and (DIM)Zn(NO₂)₂ all result in the formation of [Q + TBA]⁺ (Figures S27, S37, S31, S33, and S25). Interestingly, when comparing the bis(nitrate) and bis(nitrite) complexes for nickel, cobalt, and zinc, the TBA adduct has greater intensity for the bis(nitrite) in each case. We hypothesize that the poor σ -basicity of nitrate compared to nitrite leads to ligand loss before a TBA adduct can be formed in the spectrometer. Because nitrite is a better ligand, the TBA adduct is more likely to form instead of nitrito loss.

In contrast to the oxyanion complexes, the addition of [TBA]I to $(DIM)NiBr_2$ shows only a trace amount of TBA adduct by mass spectrometry, despite showing a large signal for TBA^+ (Figure S40). This indicates that the nitrogen oxyanions have an integral role in the formation of the TBA adducts, and cation pairing with TBA^+ may not be universal to all $(DIM)MX_2$ species. We hypothesize that the ability of the nitrogen oxyanions to engage in H-bonding with TBA^+ cation helps facilitate the adduct formation.

Origin of "Ion Tagging" of Neutrals by $N(N-Bu)_4^+$. "Noncovalent pairing" is known in ESI^{56–64} and can have diverse causes, including Bronsted or Lewis acid/base attraction and alkylammonium shape complementarity. To identify the cause of the noncovalent interaction between uncharged oxyanion complexes and TBA, we employed DFT calculations of the TBA adduct of $(DIM)Ni(NO_2)_2$.

Geometry optimization of $[(DIM)Ni(\kappa^2\text{-}ONO)_2\cdot\text{TBA}]^+$ showed the triplet spin state to be more stable than the singlet by 9.6 kcal/mol. The optimized structure (Figure 6) shows several close hydrogen-bonding contacts to nitrito O and N. The shortest (H–N at 2.28 Å) is between one butyl α -H and a nitrito nitrogen lone pair. Three other contacts are between hydrogen and oxygen, with two involving the same α -H and the last involving a β -H (2.57 Å). The α -H are the most acidic, ^{65,66} which is highlighted by the three short H-bonds. The formation of $[(DIM)Ni(ONO)_2\cdot TBA]^+$ from (DIM)Ni(ONO)₂ and TBA⁺ has a ΔG° of -14 kcal/mol, showing the collective impact of multiple weak H-bonds. There are no significant changes in N–O or C–H distances consequent from this H-bonding, and the TBA N–C–C and C–C–C angles are all conventional (109.7°–119.4°)

In an attempt to search for an alternative minimum with a different TBA interaction, geometry optimization was performed beginning with triplet (DIM)Ni(ONO)₂ where one nitrito ligand was monodentate and the TBA was interacting with the pendant oxygen with pseudo- C_3 symmetry with respect to three α -H protons. This adduct underwent a

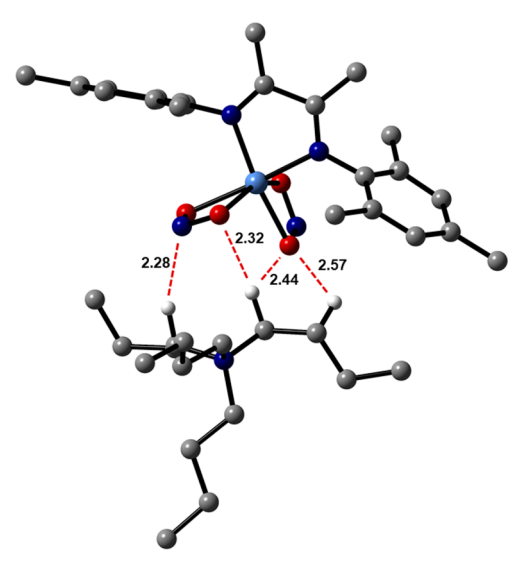


Figure 6. Optimized structure of triplet $[(DIM)Ni(κ^2-ONO)_2*TBA]^+$, showing four closest contacts to TBA hydrogens.

large structural rearrangement to yield an κ^2 -O,N-nitrite isomer, with short Ni–N and Ni–O distances, showing numerous TBA H–O or N contacts <2.9 Å. Importantly, this adduct lies only 4 kcal/mol higher in energy than the above, indicating that the PES for interaction between (DIM)Ni(κ^2 -ONO)₂ and TBA is "soft", with many competing nearly isoenergetic minima. Overall, this study explains the driving force behind this surprising N(n-butyl)₄+/neutral pairing when nitrito anions are present, even if there is no pendant oxygen.

CONCLUSIONS

This work helps provide a more holistic view of deoxygenation of bis(oxyanion) complexes of mid-to-late first row transition metals supported by a redox-active bidentate ligand. With iron, a dinitrosyl complex is formed. With cobalt and nickel, mononitrosyl complexes are isolated, and N2O is formed in the deoxygenation of nickel NO_x complexes. With zinc, no nitrosyl complexes are isolated, and NO and N2O are observed in the headspace after the reductive deoxygenations. There is a direct correlation between placement in the d-block with gaseous byproducts, and moving later in the first row (Ni, Zn) encourages N-N bond formation. We have shown that addition of NO gas to the Ni(I) bromide bridged dimer results in the formation of the mixed halogen/oxyanion complex (DIM)Ni(NO)(Br), which we use as a control in our mass spectrometry studies. The nitrogen oxyanion complexes ionize in the mass spectrometer primarily via loss of an X-type ligand, and we have observed redox chemistry at the nitrogen atom in a variety of samples. We have also shown the formation of a unique cobalt dinitrosyl dimer, which is coupled through the doubly H atom abstracted DIM ligand. The m/z for this dimer is also observed in the ESI mass spectrum of (DIM)Co(NO)(ONO), indicating its favorability over the neutral dinitrosyl monomer originally targeted. The addition of TBA allows for the observance of the intact molecular ion in most nitrogen oxyanion complexes, representing a promising synthetic procedure for characterization of the molecular complexes. Lastly, we show via DFT that H-bonding between the TBA and the nitrogen oxyanions is a crucial stabilizing factor in the adduct formation.

ASSOCIATED CONTENT

Supporting Information

The Supporting Information is available free of charge at https://pubs.acs.org/doi/10.1021/acs.inorgchem.1c02591.

Full experimental and computational details (PDF) DFT optimized structures (ZIP)

Accession Codes

CCDC 2104548–2104554 contain the supplementary crystallographic data for this paper. These data can be obtained free of charge via www.ccdc.cam.ac.uk/data_request/cif, or by emailing data_request@ccdc.cam.ac.uk, or by contacting The Cambridge Crystallographic Data Centre, 12 Union Road, Cambridge CB2 1EZ, UK; fax: +44 1223 336033.

AUTHOR INFORMATION

Corresponding Author

Kenneth G. Caulton — Department of Chemistry, Indiana University, Bloomington, Indiana 47405, United States; orcid.org/0000-0003-3599-1038; Email: caulton@indiana.edu

Authors

Daniel M. Beagan — Department of Chemistry, Indiana University, Bloomington, Indiana 47405, United States Alyssa C. Cabelof — Department of Chemistry, Indiana University, Bloomington, Indiana 47405, United States Robert Pepin — Department of Chemistry, Indiana University

Robert Pepin – Department of Chemistry, Indiana University, Bloomington, Indiana 47405, United States

Maren Pink – Department of Chemistry, Indiana University, Bloomington, Indiana 47405, United States

Veronica Carta – Department of Chemistry, Indiana University, Bloomington, Indiana 47405, United States

Complete contact information is available at: https://pubs.acs.org/10.1021/acs.inorgchem.1c02591

Notes

The authors declare no competing financial interest.

ACKNOWLEDGMENTS

This work was supported by the Indiana University Office of Vice President for research and the National Science Foundation, Chemical Synthesis Program (SYN), by Grant CHE-1955887. Support for the acquisition of the Bruker Venture D8 diffractometer through the Major Scientific Research Equipment Fund from the President of Indiana University and the Office of the Vice President for Research is gratefully acknowledged.

REFERENCES

- (1) Dodds, W. K.; Bouska, W. W.; Eitzmann, J. L.; Pilger, T. J.; Pitts, K. L.; Riley, A. J.; Schloesser, J. T.; Thornbrugh, D. J. Eutrophication of U.S. Freshwaters: Analysis of Potential Economic Damages. *Environ. Sci. Technol.* **2009**, 43 (1), 12–19.
- (2) Könneke, M.; Bernhard, A. E.; de la Torre, J. R.; Walker, C. B.; Waterbury, J. B.; Stahl, D. A. Isolation of an autotrophic ammonia-oxidizing marine archaeon. *Nature* **2005**, *437* (7058), 543–546.
- (3) Diaz, R. J.; Rosenberg, R. Spreading Dead Zones and Consequences for Marine Ecosystems. *Science* **2008**, 321 (5891), 926.
- (4) Morris, J. G. HARMFUL ALGAL BLOOMS: An Emerging Public Health Problem with Possible Links to Human Stress on the Environment. *Annu. Rev. Energy Env.* **1999**, 24 (1), 367–390.
- (5) Häder, D.-P.; Banaszak, Ä. T.; Villafañe, V. E.; Narvarte, M. A.; González, R. A.; Helbling, E. W. Anthropogenic pollution of aquatic

- ecosystems: Emerging problems with global implications. *Sci. Total Environ.* **2020**, 713, 136586.
- (6) Park, R. J.; Jacob, D. J.; Field, B. D.; Yantosca, R. M.; Chin, M. Natural and transboundary pollution influences on sulfate-nitrate-ammonium aerosols in the United States: Implications for policy. *J. Geophys. Res.* **2004**, *109*, D15.
- (7) Challagulla, S.; Tarafder, K.; Ganesan, R.; Roy, S. All that Glitters Is Not Gold: A Probe into Photocatalytic Nitrate Reduction Mechanism over Noble Metal Doped and Undoped TiO₂. *J. Phys. Chem. C* **2017**, *121* (49), 27406–27416.
- (8) Geng, Z.; Chen, Z.; Li, Z.; Qi, X.; Yang, X.; Fan, W.; Guo, Y.; Zhang, L.; Huo, M. Enhanced photocatalytic conversion and selectivity of nitrate reduction to nitrogen over AgCl/TiO₂ nanotubes. *Dalton Trans.* **2018**, *47* (32), 11104–11112.
- (9) Krasae, N.; Wantala, K. Enhanced nitrogen selectivity for nitrate reduction on Cu–nZVI by TiO₂ photocatalysts under UV irradiation. *Appl. Surf. Sci.* **2016**, *380*, 309–317.
- (10) Tawkaew, S.; Fujishiro, Y.; Yin, S.; Sato, T. Synthesis of cadmium sulfide pillared layered compounds and photocatalytic reduction of nitrate under visible light irradiation. *Colloids Surf., A* **2001**, *179* (2), 139–144.
- (11) Rosca, V.; Duca, M.; de Groot, M. T.; Koper, M. T. M. Nitrogen Cycle Electrocatalysis. *Chem. Rev.* **2009**, *109* (6), 2209–2244.
- (12) Shen, J.; Birdja, Y. Y.; Koper, M. T. M. Electrocatalytic Nitrate Reduction by a Cobalt Protoporphyrin Immobilized on a Pyrolytic Graphite Electrode. *Langmuir* **2015**, *31* (30), 8495–8501.
- (13) Teng, W.; Bai, N.; Liu, Y.; Liu, Y.; Fan, J.; Zhang, W.-x. Selective Nitrate Reduction to Dinitrogen by Electrocatalysis on Nanoscale Iron Encapsulated in Mesoporous Carbon. *Environ. Sci. Technol.* **2018**, *52* (1), 230–236.
- (14) Xu, S.; Ashley, D. C.; Kwon, H.-Y.; Ware, G. R.; Chen, C.-H.; Losovyj, Y.; Gao, X.; Jakubikova, E.; Smith, J. M. A flexible, redoxactive macrocycle enables the electrocatalytic reduction of nitrate to ammonia by a cobalt complex. *Chem. Sci.* **2018**, *9* (22), 4950–4958.
- (15) Braley, S. E.; Ashley, D. C.; Jakubikova, E.; Smith, J. M. Electrode-adsorption activates trans-[Cr(cyclam)Cl2]+ for electrocatalytic nitrate reduction. *Chem. Commun.* **2020**, *56* (4), 603–606.
- (16) Delgado, M.; Gilbertson, J. D. Ligand-based reduction of nitrate to nitric oxide utilizing a proton-responsive secondary coordination sphere. *Chem. Commun.* **2017**, *53* (81), 11249–11252.
- (17) Ford, C. L.; Park, Y. J.; Matson, E. M.; Gordon, Z.; Fout, A. R. A bioinspired iron catalyst for nitrate and perchlorate reduction. *Science* **2016**, 354 (6313), 741–743.
- (18) Elrod, L. T.; Kim, E. Lewis Acid Assisted Nitrate Reduction with Biomimetic Molybdenum Oxotransferase Complex. *Inorg. Chem.* **2018**, *57* (5), 2594–2602.
- (19) Uyeda, C.; Peters, J. C. Selective Nitrite Reduction at Heterobimetallic CoMg Complexes. *J. Am. Chem. Soc.* **2013**, *135* (32), 12023–12031.
- (20) Gwak, J.; Ahn, S.; Baik, M.-H.; Lee, Y. One metal is enough: a nickel complex reduces nitrate anions to nitrogen gas. *Chem. Sci.* **2019**, *10* (18), 4767–4774.
- (21) Marks, W. R.; Baumgardner, D. F.; Reinheimer, E. W.; Gilbertson, J. D. Complete denitrification of nitrate and nitrite to N2 gas by samarium(ii) iodide. *Chem. Commun.* **2020**, *56* (77), 11441–11444
- (22) Khin, C.; Heinecke, J.; Ford, P. C. Oxygen Atom Transfer from Nitrite Mediated by Fe(III) Porphyrins in Aqueous Solution. *J. Am. Chem. Soc.* **2008**, *130* (42), *13830*–13831.
- (23) Kulbir; Das, S.; Devi, T.; Goswami, M.; Yenuganti, M.; Bhardwaj, P.; Ghosh, S.; Chandra Sahoo, S.; Kumar, P. Oxygen atom transfer promoted nitrate to nitric oxide transformation: a step-wise reduction of nitrate nitrite nitric oxide. *Chem. Sci.* **2021**, *12* (31), 10605–10612.
- (24) Kundu, S.; Kim, W. Y.; Bertke, J. A.; Warren, T. H. Copper(II) Activation of Nitrite: Nitrosation of Nucleophiles and Generation of NO by Thiols. *J. Am. Chem. Soc.* **2017**, *139* (3), 1045–1048.

- (25) Beagan, D. M.; Huerfano, I. J.; Polezhaev, A. V.; Caulton, K. G. Reductive Silylation Using a Bis-silylated Diaza-2,5-cyclohexadiene. *Chem. Eur. J.* **2019**, 25 (34), 8105–8111.
- (26) Beagan, D. M.; Carta, V.; Caulton, K. G. A reagent for heteroatom borylation, including iron mediated reductive deoxygenation of nitrate yielding a dinitrosyl complex. *Dalton Trans.* **2020**, 49 (5), 1681–1687.
- (27) Seo, J.; Cabelof, A. C.; Chen, C.-H.; Caulton, K. G. Selective deoxygenation of nitrate to nitrosyl using trivalent chromium and the Mashima reagent: reductive silylation. *Chem. Sci.* **2019**, *10* (2), 475–470
- (28) Cabelof, A. C.; Carta, V.; Caulton, K. G. A proton-responsive ligand becomes a dimetal linker for multisubstrate assembly via nitrate deoxygenation. *Chem. Commun.* **2021**, *57*, 2780–2783.
- (29) Beagan, D. M.; Cabelof, A. C.; Pink, M.; Carta, V.; Gao, X.; Caulton, K. G. Nickel-mediated N–N bond formation and N2O liberation via nitrogen oxyanion reduction. *Chem. Sci.* **2021**, *12*, 10664–10672.
- (30) Gonsalvi, L.; Gaunt, J. A.; Adams, H.; Castro, A.; Sunley, G. J.; Haynes, A. Quantifying Steric Effects of α-Diimine Ligands. Oxidative Addition of MeI to Rhodium(I) and Migratory Insertion in Rhodium(III) Complexes. *Organometallics* **2003**, 22 (5), 1047–1054.
- (31) Bart, S. C.; Hawrelak, E. J.; Schmisseur, A. K.; Lobkovsky, E.; Chirik, P. J. Synthesis, Reactivity, and Solid State Structures of Four-Coordinate Iron(II) and Manganese(II) Alkyl Complexes. *Organometallics* **2004**, 23 (2), 237–246.
- (32) Kiernicki, J. J.; Higgins, R. F.; Kraft, S. J.; Zeller, M.; Shores, M. P.; Bart, S. C. Elucidating the Mechanism of Uranium Mediated Diazene N-N Bond Cleavage. *Inorg. Chem.* **2016**, *55* (22), 11854–11866.
- (33) Victor, E.; Kim, S.; Lippard, S. J. Synthesis of Bis(imidazole) Metal Complexes and Their Use in Rapid NO Detection and Quantification Devices. *Inorg. Chem.* **2014**, *53* (24), 12809–12821.
- (34) Plakatouras, J. C.; Perlepes, S. P.; Mentzafos, D.; Terzis, A.; Bakas, T.; Papaefthymiou, V. Coordination chemistry of corrosion inhibitors of the benzotriazole type: Preparation and characterization of cobalt(II) complexes with 1-methylbenzotriazole (Mebta) and the crystal structures of [CoCl2(Mebta)2], trans-[Co(NCS)2 (Mebta)4], trans-[Co(NCS)2(MeOH)2(Mebta)2] and cis-[Co(NO3)2(Mebta)2]. *Polyhedron* 1992, 11 (20), 2657–2672.
- (35) Kriley, C. E.; Majireck, M. M.; Tobolewski, J. M.; Kelvington, L. E.; Cummings, S. H.; Hershberger, S. J.; Link, J. D.; Silverio, A. L.; Fanwick, P. E.; Rothwell, I. P. Synthesis and characterization of two novel cobalt (II) phosphine complexes: crystal structures of [CoCl3(Cy2PCH2PCy2H)] and [Co(NO3)2(Cy2PCH2PCy2O)]. Cy = cyclohexyl, C6H11. *Inorg. Chim. Acta* **2005**, 358 (1), 57–62.
- (36) Toscano, P. J.; Belsky, K. A.; Engelhardt, L. M.; Fordon, K. J.; White, A. H. Improved synthesis and isolation of a flexible linear NSNN tetradentate ligand and the crystal structure of its stereospecific dinitrocobalt(III) complex. *Inorg. Chem.* **1990**, 29 (7), 1357–1359.
- (37) Xu, S.; Kwon, H.-Y.; Ashley, D. C.; Chen, C.-H.; Jakubikova, E.; Smith, J. M. Intramolecular Hydrogen Bonding Facilitates Electrocatalytic Reduction of Nitrite in Aqueous Solutions. *Inorg. Chem.* **2019**, *58* (14), 9443–9451.
- (38) Otter, C. A.; Hartshorn, R. M. Preparation and photochemistry of cobalt(iii) amino and amino acidato complexes containing tripodal polypyridine ligands. *Dalton Trans.* **2004**, No. 1, 150–156.
- (39) Downward, A. M.; Polson, M. I. J.; Kerr, W. R.; Kariyawasam, J.; Hartshorn, R. M. Synthesis of a nitrogen mustard ligand on a cobalt(III) metal centre. *Polyhedron* **2013**, *52*, 617–622.
- (40) Crimmin, M. R.; Rosebrugh, L. E.; Tomson, N. C.; Weyhermüller, T.; Bergman, R. G.; Toste, F. D.; Wieghardt, K. [(TMEDA)Co(NO)2][BPh4]: A versatile synthetic entry point to four and five coordinate {Co(NO)2}10 complexes. *J. Organomet. Chem.* **2011**, 696 (25), 3974–3981.
- (41) Deka, H.; Ghosh, S.; Saha, S.; Gogoi, K.; Mondal, B. Effect of ligand denticity on the nitric oxide reactivity of cobalt(ii) complexes. *Dalton Trans.* **2016**, 45 (27), 10979–10988.

- (42) Gerbase, A. E.; Vichi, E. J. S.; Stein, E.; Amaral, L.; Vasquez, A.; Hörner, M.; Maichle-Mössmer, C. Preparation, characterization and electrochemical studies of 1,1'-bis(diphenylphosphino) ferrocene (dppf) derivatives. Crystal structure of [dppfCo(NO)2][SbF6]. *Inorg. Chim. Acta* 1997, 266 (1), 19–27.
- (43) Kaduk, J. A.; Ibers, J. A. Structure of dinitrosyl(1,2-bis(diphenylphosphino)ethane)cobalt hexafluorophosphate, [Co-(NO)2((C_6H_5)2PC2H4P(C_6H_5)2)][PF6]. *Inorg. Chem.* **1977**, 16 (12), 3283–3287.
- (44) Tennyson, A. G.; Dhar, S.; Lippard, S. J. Synthesis and Characterization of {Ni(NO)}10 and {Co(NO)2}10 Complexes Supported by Thiolate Ligands. J. Am. Chem. Soc. 2008, 130 (45), 15087–15098.
- (45) Tomson, N. C.; Crimmin, M. R.; Petrenko, T.; Rosebrugh, L. E.; Sproules, S.; Boyd, W. C.; Bergman, R. G.; DeBeer, S.; Toste, F. D.; Wieghardt, K. A Step beyond the Feltham–Enemark Notation: Spectroscopic and Correlated ab Initio Computational Support for an Antiferromagnetically Coupled M(II)–(NO)- Description of Tp*M-(NO) (M = Co, Ni). *J. Am. Chem. Soc.* **2011**, *133* (46), 18785–18801.
- (46) Fujisawa, K.; Soma, S.; Kurihara, H.; Dong, H. T.; Bilodeau, M.; Lehnert, N. A cobalt–nitrosyl complex with a hindered hydrotris(pyrazolyl)borate coligand: detailed electronic structure, and reactivity towards dioxygen. *Dalton Trans.* **2017**, *46* (39), 13273–13289.
- (47) Stirling, A.; Pápai, I.; Mink, J.; Salahub, D. R. Density functional study of nitrogen oxides. *J. Chem. Phys.* **1994**, *100* (4), 2910–2923.
- (48) Bard, A. J.; Faulkner, L. J. Electrochemical Methods: Fundamentals and Applications. John Wiley & Sons: New York; 2000.
- (49) Zarate, C.; Yang, H.; Bezdek, M. J.; Hesk, D.; Chirik, P. J. Ni(I)—X Complexes Bearing a Bulky α -Diimine Ligand: Synthesis, Structure, and Superior Catalytic Performance in the Hydrogen Isotope Exchange in Pharmaceuticals. *J. Am. Chem. Soc.* **2019**, *141* (12), 5034–5044.
- (50) Wright, A. M.; Zaman, H. T.; Wu, G.; Hayton, T. W. Mechanistic Insights into the Formation of N2O by a Nickel Nitrosyl Complex. *Inorg. Chem.* **2014**, *53* (6), 3108–3116.
- (51) Moore, C. M.; Szymczak, N. K. Nitrite reduction by copper through ligand-mediated proton and electron transfer. *Chem. Sci.* **2015**, *6* (6), 3373–3377.
- (52) Petel, B. E.; Matson, E. M. Conversion of NOx1- (x = 2, 3) to NO using an oxygen-deficient polyoxovanadate—alkoxide cluster. *Chem. Commun.* **2020**, *56* (4), 555–558.
- (53) Mondal, A.; Reddy, K. P.; Bertke, J. A.; Kundu, S. Phenol Reduces Nitrite to NO at Copper(II): Role of a Proton-Responsive Outer Coordination Sphere in Phenol Oxidation. *J. Am. Chem. Soc.* **2020**, *142* (4), 1726–1730.
- (54) Hojilla Atienza, C. C.; Milsmann, C.; Semproni, S. P.; Turner, Z. R.; Chirik, P. J. Reversible Carbon—Carbon Bond Formation Induced by Oxidation and Reduction at a Redox-Active Cobalt Complex. *Inorg. Chem.* **2013**, *52* (9), 5403—5417.
- (55) Esposito, R.; Calvanese, L.; Cucciolito, M. E.; D'Auria, G.; Falcigno, L.; Fiorini, V.; Pezzella, P.; Roviello, G.; Stagni, S.; Talarico, G.; Ruffo, F. Oxidative Coupling of Imino, Amide Platinum(II) Complexes Yields Highly Conjugated Blue Dimers. *Organometallics* 2017, 36 (2), 384–390.
- (56) McIndoe, J. S.; Vikse, K. L. Assigning the ESI mass spectra of organometallic and coordination compounds. *J. Mass Spectrom.* **2019**, 54 (5), 466–479.
- (57) Sessler, J. L.; Gross, D. E.; Cho, W.-S.; Lynch, V. M.; Schmidtchen, F. P.; Bates, G. W.; Light, M. E.; Gale, P. A. Calix[4]pyrrole as a Chloride Anion Receptor: Solvent and Countercation Effects. J. Am. Chem. Soc. 2006, 128 (37), 12281–12288.
- (58) Gross, D. E.; Schmidtchen, F. P.; Antonius, W.; Gale, P. A.; Lynch, V. M.; Sessler, J. L. Cooperative Binding of Calix[4]pyrrole—Anion Complexes and Alkylammonium Cations in Halogenated Solvents. *Chem. Eur. J.* **2008**, *14* (26), 7822–7827.

- (59) Kodiah Beyeh, N.; Göth, M.; Kaufmann, L.; Schalley, C. A.; Rissanen, K. The Synergetic Interplay of Weak Interactions in the Ion-Pair Recognition of Quaternary and Diquaternary Ammonium Salts by Halogenated Resorcinarenes. *Eur. J. Org. Chem.* **2014**, 2014 (1), 80–85.
- (60) Mansikkamäki, H.; Schalley, C. A.; Nissinen, M.; Rissanen, K. Weak interactions between resorcinarenes and diquaternary alkyl ammonium cations. *New J. Chem.* **2005**, 29 (1), 116–127.
- (61) Mansikkamäki, H.; Nissinen, M.; Schalley, C. A.; Rissanen, K. Self-assembling resorcinarene capsules: solid and gas phase studies on encapsulation of small alkyl ammonium cations. *New J. Chem.* **2003**, 27 (1), 88–97.
- (62) Frański, R.; Gierczyk, B. Unusual complex between 18-Crown-6 and tetramethylammonium cation—detection by electrospray ionization mass spectrometry. *J. Inclusion Phenom. Mol. Recognit. Chem.* **2008**, *62* (3), 339–343.
- (63) Åhman, A.; Luostarinen, M.; Rissanen, K.; Nissinen, M. Complexation of C-methyl pyrogallarene with small quaternary and tertiary alkyl ammonium cations. *New J. Chem.* **2007**, *31* (1), 169–177
- (64) Schalley, C. A.; Castellano, R. K.; Brody, M. S.; Rudkevich, D. M.; Siuzdak, G.; Rebek, J. Investigating Molecular Recognition by Mass Spectrometry: Characterization of Calixarene-Based Self-Assembling Capsule Hosts with Charged Guests. *J. Am. Chem. Soc.* 1999, 121 (19), 4568–4579.
- (65) Reetz, M. T.; Hütte, S.; Goddard, R. Supramolecular structure of the tetrabutylammonium salt of 2-phenylpropionitrile. *J. Prakt. Chem.* **1999**, 341 (3), 297–301.
- (66) Shirakawa, S.; Liu, S.; Kaneko, S.; Kumatabara, Y.; Fukuda, A.; Omagari, Y.; Maruoka, K. Tetraalkylammonium Salts as Hydrogen-Bonding Catalysts. *Angew. Chem., Int. Ed.* **2015**, *54* (52), 15767–15770